The Canadian Mineralogist
Vol. 49, pp. 503-520 (2011)
DOI: 10.3749/canmin.49.2.503

DAWSONITE IN TUFFS AND LITHARENITES OF THE CERRO CASTAÑO MEMBER, CERRO BARCINO FORMATION, CHUBUT GROUP (CENOMANIAN), LOS ALTARES, PATAGONIA, ARGENTINA

PATRICIA EUGENIA ZALBA

Comisión de Investigaciones Científicas provincia de Buenos Aires (CIC) – Centro de Tecnología de Recursos Minerales y Cerámica (CETMIC–CIC–CONICET), C. C. 49, Manuel B. Gonnet (B1897ZCA), Argentina and School of Geosciences, Monash University, Melbourne, Australia

MARÍA SUSANA CONCONI§

Comisión de Investigaciones Científicas provincia de Buenos Aires (CIC) – Centro de Tecnología de Recursos Minerales y Cerámica (CETMIC–CIC–CONICET), C. C. 49, Manuel B. Gonnet (B1897ZCA), Argentina and Facultad de Ingeniería (UNLP), La Plata, Argentina

MARTÍN MOROSI

Comisión de Investigaciones Científicas provincia de Buenos Aires (CIC) – Centro de Tecnología de Recursos Minerales y Cerámica (CETMIC–CIC–CONICET), C. C. 49, Manuel B. Gonnet (B1897ZCA), Argentina and Facultad de Ciencias Naturales y Museo de La Plata (UNLP), Argentina

MARCELO MANASSERO

Facultad de Ciencias Naturales y Museo de La Plata (UNLP), Argentina and Consejo Nacional de Investigaciones Científicas y Técnicas (CONICET) – Centro de Investigaciones Geológicas (CIG), Calle 1 No. 644, (1900) La Plata, Argentina

MARCOS COMERIO

Comisión de Investigaciones Científicas provincia de Buenos Aires (CIC) – Centro de Tecnología de Recursos Minerales y Cerámica (CETMIC–CIC–CONICET), C. C. 49, Manuel B. Gonnet (B1897ZCA), Argentina

ABSTRACT

Dawsonite, $NaAlCO_3(OH)_2$, occurs as a replacement, cement, and fracture filling in continental, zeolitized and silicified vitric tuffs and litharenites of the Cenomanian Cerro Castaño Member, Cerro Barcino Formation, Chubut Group, Patagonia, Argentina. Analcime is the only associated zeolite; it replaces the vitric masses and also fills fractures and cavities. Dawsonite and analcime display an inverse ratio. Textural relationships indicate that dawsonite is a pseudomorph after oligoclase, quartz, vitric shards, and vitric masses; it coexists with diagenetic quartz cement and postdates analcime, calcite, and hematite cements. Unaltered crystals of high sanidine postdate all other cements generated. Silicification of the tuffs is likely to have occurred in various stages during the diagenetic history of the sequence. Hypabyssal bodies of alkaline basic rocks of the El Buitre – El Canquel Formation, which intruded regionally the Cerro Castaño Member during Eocene time, are interpreted to be responsible for the introduction of CO_2 gas at high partial pressures, together with sodium, which led to dawsonite formation. Diagenetic quartz, at a late stage of silicification, is related to the transformation of oligoclase and analcime to dawsonite, also releasing Na and Ca into the system. The $\delta^{13}C$ (PDB) values of dawsonite, in the range –1.2 to –2.4‰, attest to alkaline igneous activity in the Cerro Castaño Member during the Eocene and, in addition, set a limit on the age of the dawsonite.

Keywords: dawsonite, Chubut Group, Cenomanian, diagenesis, magmatic CO_2, paragenetic sequence, Patagonia, Argentina.

§ *E-mail address*: msconconi@cetmic.unlp.edu.ar

Sommaire

On trouve la dawsonite, $NaAlCO_3(OH)_2$, comme remplacement, comme ciment, et en remplissage de fissures dans des tufs continentaux zéolitisés et silicifiés et dans les litharénites d'âge cénomanien du Membre de Cerro Castaño, Formation de Cerro Barcino, Groupe de Chubut, en Patagonie, Argentine. L'analcime, la seule zéolite associée, remplace les masses vitreuses et remplit aussi les fissures et les cavités. La quantité de dawsonite et celle d'analcime montrent un rapport inverse. D'après les relations texturales, la dawsonite remplace l'oligoclase, le quartz, les esquilles de verre et les masses vitreuses. Elle coexiste avec le quartz diagénétique et s'est formée après l'analcime, la calcite et l'hématite. Des cristaux sains de sanidine désordonnée sont apparus après tous les autres ciments. Il est probable que la silicification des tufs a eu lieu en plusieurs étapes au cours de l'évolution diagénétique de la séquence de tufs. Des venues hypabyssales de roches basiques alcalines de la Formation de El Buitre – El Canquel, qui ont recoupé sur une échelle régionale le Membre de Cerro Castaño durant l'Éocène, seraient responsables de l'introduction du CO_2 à une pression partielle élevée avec le sodium, ce qui a mené à la formation de la dawsonite. Le quartz diagénétique, à un stade tardif de la silicification, est lié à la transformation de l'oligoclase et de l'analcime à la dawsonite, ce qui a aussi contribué le Na et le Ca au système. Les valeurs de $\delta^{13}C$ (PDB) de la dawsonite, dans l'intervalle –1.2 à –2.4‰, témoignent de l'activité ignée alcaline dans le Membre de Cerro Castaño au cours de l'Éocène et, de plus, placent une limite sur l'âge de la dawsonite.

(Traduit par la Rédaction)

Mots-clés: dawsonite, Groupe de Chubut, âge cénomanien, diagenèse, CO_2 magmatique, séquence paragénétique, Patagonie, Argentine.

Introduction

Dawsonite, a basic carbonate of sodium and aluminum, $NaAlCO_3(OH)_2$, was encountered for the first time in Argentina in the Cretaceous pyroclastic sequences of the Cerro Castaño Member, Cerro Barcino Formation, Chubut Group, northern Patagonia. The objective of this contribution is the full characterization of dawsonite through optical and electron microscopy, X-ray diffraction, chemical and thermogravimetric analyses, and stable isotope data. This characterization was possible on account of the abundant, pure, well-developed crystals occurring in outcrops of fine-grained vitric tuffs and litharenites of this unit.

Two mentions of dawsonite have been made in South America. The first one was in Argentina, where birefringent crystals contained in fluid inclusions were inferred to be "possible dawsonite" by Domínguez & Gómez (1988) in the Serie Andacollo, Neuquén, northern Patagonia, but the authors could not characterize it. The second mention was made in Bolivia, Cerro Sapo locality, where it was characterized by X-ray diffraction, infrared and Raman spectroscopy and chemical analysis (http://rruff.info. Dawsonite: RRUFF ID: R050645).

Taking into account that diverse occurrences of dawsonite in sedimentary rocks are found all over the world and include diagenetic assemblages (Smith & Milton 1966, Loughnan & See 1967, Hay 1963, 1964, Goldbery & Loughnan 1970, 1977, Baker 1991, Baker *et al*. 1995, Worden 2006, among others), we believe that the genesis of the dawsonite within these pyroclastic rocks is undoubtedly related to these processes. Also, we propose the timing of its formation, associated with the emplacement of recent and neighboring igneous intrusive bodies, previously described in the study area; these rocks were the main source of Na and CO_2.

Geological Setting

The continental Cretaceous Chubut Group, found in the San Jorge Basin, one of the five most important oil-producing fields in Argentina, extends along the border between the Chubut and Santa Cruz provinces in a north–south direction and from the Argentinean continental platform to the Cordillera de Los Andes, in an east–west direction (Fitzgerald *et al*. 1990, Anselmi *et al*. 2004, Cladera *et al*. 2004). The sequences of the Chubut Group have been described by Volkheimer (1969), Robbiano (1971), Musacchio & Chebli (1975), and Codignotto *et al*. (1978), among others. The geology of the Paso de Indios – Las Plumas area is displayed in Figure 1, adapted from Codignotto *et al*. (1978). The Chubut Group, which attains a total thickness of 1000 m, was mapped by Lesta & Ferello (1972) and Chebli *et al*. (1976), among many others, and, in our area comprises the Los Adobes and the Cerro Barcino formations (Fig. 1). The Cerro Barcino Formation comprises five volcaniclastic members which, from bottom to top, are: Puesto La Paloma, Cerro Castaño, Las Plumas and Puesto Manuel Arce – Bayo Overo (lateral facies). The Cerro Castaño (90 m) and the Las Plumas (90 m) members are the most widespread sequences along the Middle Chubut Valley River.

The Cerro Barcino Formation lies unconformably over Jurassic volcanic and sedimentary deposits and also over Proterozoic and lower Paleozoic metamorphic and igneous basement rocks. The Triassic and Jurassic periods were characterized by crustal extension processes (Gondwana break-up). Structurally, continental upper Triassic sediments are disposed in

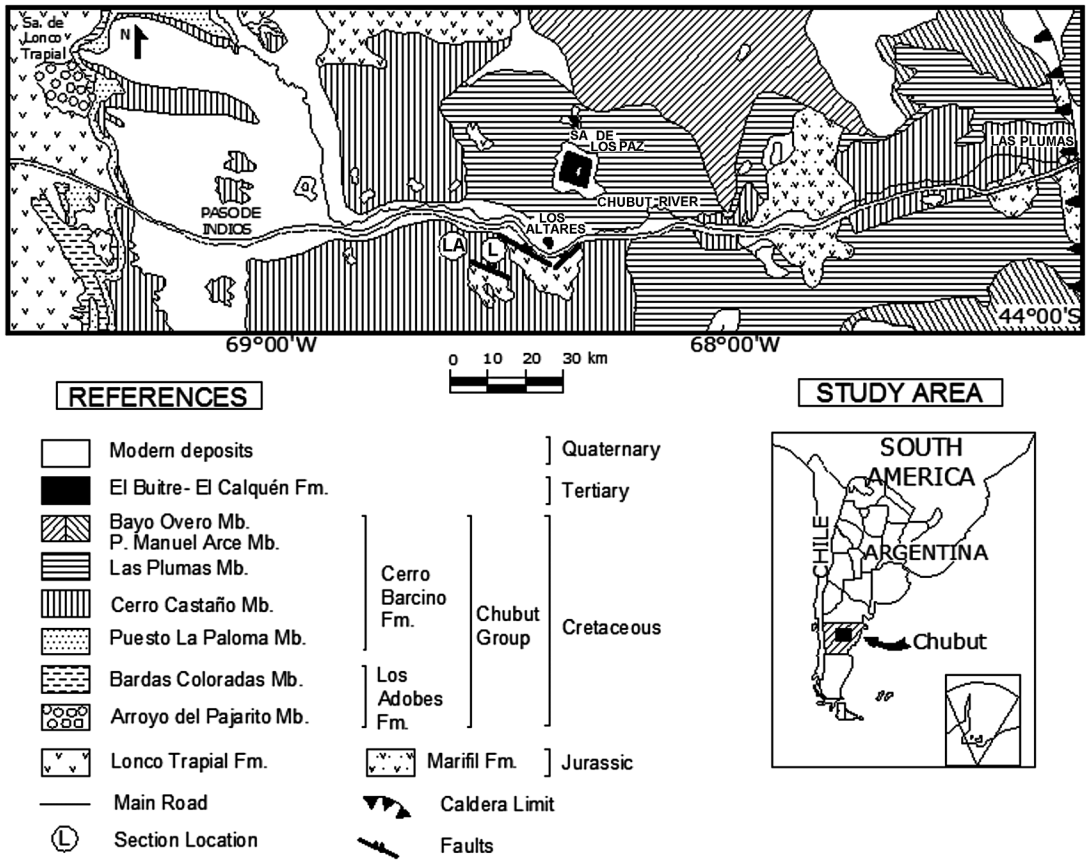

FIG. 1. Geological map (adapted from Codignotto *et al*. 1978) showing the location of the sections studied and the simplified stratigraphic scheme of the Chubut Group in the study area.

intracratonic subparallel basins (semigraben systems). During the middle to upper Jurassic, a back-arc basin appeared to the east of the continental volcanic arc (Anselmi *et al*. 2004).

The age of the Chubut Group is considered Barremian–Cenomanian on the basis of biostratigraphic data from charofites and ostracoda of the Puesto La Paloma Member (Musacchio 1972, Musacchio & Chebli 1975). Codignotto *et al*. (1978) and Manassero (1997) correlated the upper part of this group with the Angostura Colorada Formation (Coniacian–Campanian) cropping out 300 km to the northwest of the study area. A marine ingression occurred to the west of the basin (Thitonian). With the withdrawal of the sea, the deposition of the Chubut Group began, and the first basin inversion occurred (Barcat *et al*. 1989), accompanied by compressive phenomena that generated the folding of the sequences.

In the Paleogene (Eocene), the Cerro Barcino Formation was intruded by basic, alkaline hypabyssal bodies of the El Buitre – El Canquel Formation (Lema & Cortés 1987, Anselmi *et al*. 2000) composed of alkali basalt, diabase, basanite, teshenite and gabbro. These magmatic bodies were emplaced at high levels of the crust, in a back-arc environment (Ardolino *et al*. 1995), corresponding to magmatism related with extensional processes of the intraplate rift type. The gabbros bear "*analcime, possible natrolite, and medium to sodium labradorite*" (Fernández 2000). Several exposures of the El Buitre – El Canquel Formation have been mapped less than 10 km northwest and east of the study area, including the important Sierra de Los Paz (Anselmi *et al*. 2004). From Neogene time, intraplate volcanism led to an outpouring of basaltic lavas related to a hot spot (Kay *et al*. 1993).

The five members of the Cerro Barcino Formation were previously studied in the Middle Chubut River Valley (Paso de Indios – Los Altares – Las Plumas) by Iñíguez Rodríguez *et al*. (1987). The authors defined four vertical different zones in a sequence of pyroclastic

and epiclastic rocks 300 m thick, with analcime at the base (Puesto La Paloma Member), analcime–clinoptilolite in the middle part (Cerro Castaño Member), clinoptilolite (Las Plumas Member) and glass at the top (Puesto Manuel Arce – Bayo Overo members). A diagenetic origin for these minerals was proposed by these authors and related to ash falls deposited in flat plains with saline–alkaline lakes, later affected by burial diagenesis, responsible for the vertical zonation of the zeolites. No dawsonite was detected by the authors.

Manassero *et al.* (1998, 2000) studied the distribution, paleoenvironmental conditions of deposition and mineralogy of the Cerro Castaño and the Las Plumas members of the Cerro Barcino Formation along the Chubut River, between Los Altares and Las Plumas localities, and postulated the existence of syneruptive and intereruptive facies for these sediments. According to these authors, pyroclastic sediments (ash falls) covered extensive flats or slightly undulating plains with shallow ponds and poorly developed drainage systems flowing to the north–northeast. The abundance of fine planar and cuspate shards in the tuffs suggested that the explosive center was probably located approximately 500 km to the west of the study area.

Methodology

Twenty-seven samples of tuff and one sample of litharenite from two stratigraphic sections of the Cerro Castaño Member (Fig. 2, sections L and LA) were studied by optical microscopy and X-ray diffraction (XRD). Dawsonite was easily hand-picked from the surface of the rock by the use of a fine needle and observed under a stereomicroscope. Very pure material was recovered for chemical analysis, performed by inductively coupled plasma – atomic emission spectroscopy technique (ICP–AES), X-ray powder diffraction, simultaneous differential thermal and thermogravimetric analysis (DTA–TG) and scanning electron microscopy (SEM).

Crystalline phases were identified and quantified by X-ray diffraction with a Philips 3020 goniometer (Ni-filtered Cu$K\alpha$ radiation, 40 kV, 20 mA, without secondary monochromator). Step-scan data were collected from 3° to 70° 2θ, with a step width of 0.04° and a counting time of 2 s/step. Samples with a high iron content were analyzed using special conditions (base level of the Pulse Height Discriminator in the X-ray detector system set at 45°). The hand-picked sample of dawsonite was scanned between 8° and 70°, with a step width of 0.02° and a step-counting time of 2 seconds.

The powder-diffraction patterns were analyzed with the FullProf program, which is a multipurpose profile-fitting program, including Rietveld refinement (Rodríguez Carvajal 2001). A Rietveld analysis (Rietveld 1969) was used for cell-parameter calculation of hand-picked dawsonite and for quantitative determination of the crystalline phases for samples from sections L and LA. The starting crystallographic data used for each phase were extracted from the literature.

The DTA–TG analysis was carried out in open PtRh crucibles in air. The sample was heated up to 1000°C at a heating rate of 10°C/minute using a Netzsch STA 409c equipment. The texture and mineralogical composition of the sediments were examined using a Jeol JSM 5800 scanning electron microscope.

Six different samples of pure dawsonite were analyzed for their C and O isotope values in two different laboratories. Five analyses were performed at the Instituto de Geocronología y Geología Isotópica (INGEIS), CONICET – Universidad de Buenos Aires, Argentina. The technique was based on the method developed by McCrea (1950), with slight modifications. The CO_2 fraction was extracted by reaction with phosphoric acid at 60°C during two hours, purified in a high-vacuum line, and analyzed with a mass spectrometer (Delta S Finnigan Mat triple collector). The $\delta^{13}C$ and $\delta^{18}O$ values were reported in ‰, relative to the standard V–PDB (Vienna Pee Dee Belemnitella) (Coplen 1994). Values of $\delta^{18}O$ are also expressed with respect to the V–SMOW (Vienna Standard Mean Ocean Water). The analytical error was 0.1‰ ($\pm 2\sigma$) for $\delta^{13}C$ and $\delta^{18}O$.

One more sample was analyzed at the Laboratorio de Isotopos Estáveis (LABISE), Department of Geology, Universidade Federal de Pernambuco, Recife, Brazil. The extraction of CO_2 was performed with orthophosphoric acid at 25°C for one day. The released CO_2 was analyzed in a double-inlet, triple-collector SIRA II mass spectrometer, and results are reported relative to the PDB (Pee Dee Belemnitella) standard. Values of $\delta^{18}O$ are expressed with respect to the SMOW (Standard Mean Ocean Water).The uncertainties of the isotope measurement were better than 0.1‰ for carbon and 0.2‰ for oxygen.

Results

The Cerro Castaño Member: stratigraphic sections

The Cerro Castaño Member is composed of tabular brownish, yellowish to whitish tuffs that are widespread on both margins of the Middle Valley of the Chubut River. The outcrops studied here comprise zeolitized and silicified tuffs, sandstones and conglomerates, which extend along the right margin of the Chubut River, to the west of the Los Altares locality.

Two stratigraphic sections (Fig. 2) show the presence of dawsonite: Section L (70 m thick) composed of abundant tuffs and minor sandstones, and Section LA (110 m thick), 5 km to the southwest of Section L, in which sandstones and conglomerates are more abundant, and which bears microscopic vertebrate remains.

The tuffs of the Cerro Castaño Member show dominant pale yellow-brown colors; the strata are exposed in steep ridges (Fig. 3a). Tabular beds are one to two

meters thick and show sharp basal contacts. Most of the strata are massive. Fine-grained vitric tuffs are dominant over litharenites.

Dawsonite occurs in tuffs as coalescent aggregates of radiating acicular crystals (Fig. 3b), whitish in color, though they are commonly colored by ferric oxides filling fractures and microfractures. Dawsonite is very abundant at the surface, mainly where the tuffs are protected by overhanging strata, as mentioned in the literature (Goldbery & Loughnan 1970).

Petrology and mineralogy

The pyroclastic rocks of the Cerro Castaño Member plot in the tuff field (Fig. 4a) in a diagram adapted from Fisher & Schmincke (1984). The composition of the fluvial interbedded sandstones plots in the triangular diagram of Folk *et al*. (1970) where feldspathic litharenites are dominant, in accordance with the findings of Manassero *et al*. (2000) (Fig. 4b). The Cerro Castaño Member rocks show a quartzofeldspathic composition. The components of both the sandstones and the tuffs are euhedral crystals of quartz with embayments, sanidine, oligoclase (An_{25}), and fragments of volcanic material (felsic and silicified rhyolites, tuffs and andesites), and sedimentary rocks.

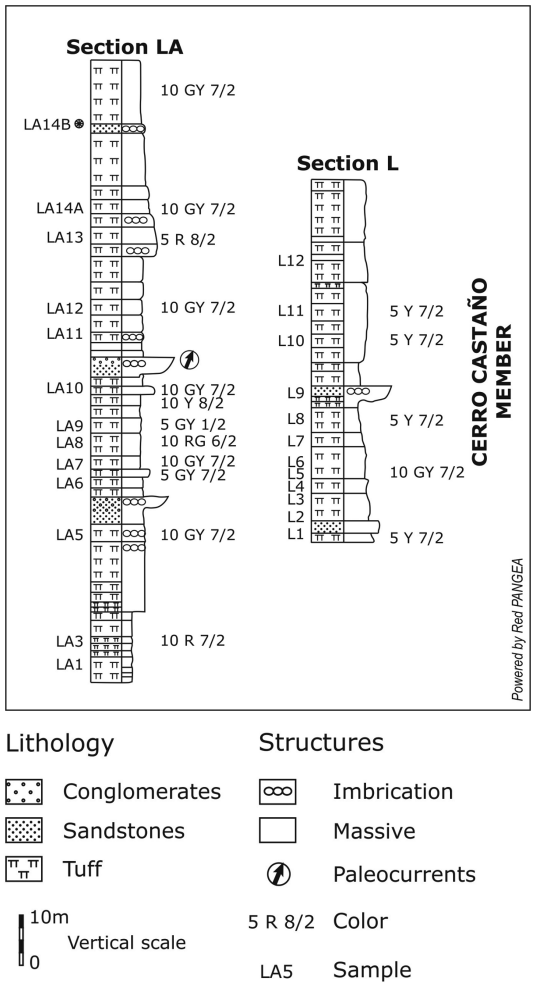

FIG. 2. Stratigraphic sections, Cerro Castaño Member, Los Altares.

The tuffs of the Cerro Castaño Member are mainly vitric. Planar and cuspate glass shards predominate over Y-shaped shards, whereas pumice fragments are very scarce. Glass shards commonly show replacement by dawsonite. Oligoclase (An_{25}), mainly with albite twinning, is fresh or has been totally or partially replaced by dawsonite or, seldom, by calcite.

The K-feldspar population shows euhedral unaltered and unzoned sanidine crystals in thin sections. Euhedral, prismatic crystals of K-feldspar (4–10 μm) have been detected by scanning electron microscopy (Fig. 5) in the altered vitric mass. Cell parameters obtained by X-ray diffraction for the K-feldspar (up to 60°, Table 1a) corresponds to high sanidine [*a* 8.5961(2), *b* 13.0133(2), *c* 7.1748(1) Å, β 116.005(1)°].

Unit-cell parameters values were plotted on the *a*-contoured *b*–*c* quadrilateral of Wright & Stewart (1968) to estimate the structural state and detect anomalous unit cells. The *a* value plots slightly outside the range of the series maximum microcline – high sanidine, and the other cell parameters fall in the vicinity of sideline high albite – high sanidine. The slight deviation observed with respect to the Or sideline (*a* 8.5961 Å) attests to very limited extent of cation substitution (Martin 1971, Kastner 1971).

Results of quantitative analyses by the Rietveld method for sections LA and L are shown in Table 1a and Table 1b. The Rwp values obtained are in accordance with typical values for XRD refinements (Bish & Post 1993). For Sections L, Rwp ranges from 20.1 to 25.3, and for Sections LA, it ranges from 17.1 to 26.2, except for sample LA14b, which shows a value of 36.6. The last sample contains almost 47% hematite, and the background is very high, even using special settings of the diffractometer for iron-rich samples. Also for this sample, the Brindley particle-absorption-contrast factor was used to correct mass abundance of the phase.

Primary quartz grains are in some cases embayed and also have been partially replaced by calcite or dawsonite (Fig. 6a). Flexured and partially bleached detrital biotite is present in all the samples but one of Section L. Section LA contains minor amounts of biotite (Table 1a), in some cases only detected in thin section.

Authigenic minerals, besides dawsonite, include: analcime, calcite, hematite, halite, trona, quartz and high sanidine. Chlorite, carbonate-rich fluorapatite and dolomite also have been identified as scarce accesories (Tables 1a, 1b).

Analcime is the only zeolite found in these two sections of the Cerro Castaño Member, although some subordinate clinoptilolite-Na has also been found in nearby areas (Iñíguez Rodríguez *et al*. 1987, 1992, Manassero *et al*. 2000, Cladera *et al*. 2004). From thin section observations, analcime occurs as euhedral crystals in pores (Fig. 6b) or fills cavities or cracks (Fig. 6c). Textural relationships show that analcime is surrounded by calcite cement (Fig. 6d).

From SEM observations, analcime shows polyhedral forms. The average size (5 μm) and distribution of analcime crystals in the altered vitric mass are shown in Figure 7a. Quantitative analyses attest to the presence of very abundant analcime (up to 52%) in almost all the samples of Section L. On the contrary, in Section LA, according to X-ray-diffraction data (Table 1a), analcime is present only in some samples and in much lower proportions (maximum 13%). Although smectite has not been detected in these samples, its presence in the Cerro Castaño Member has been reported by Iñíguez Rodríguez *et al*. (1987) as a coating that preceded the development of analcime, as a replacement of glass shards, and as a filling of available pore-space, showing a honeycomb texture.

In some cases, although calcite has not been detected by X-ray diffraction (Tables 1a, 1b), it has been identified in a petrographic analysis. It appears as euhedral sparitic calcite cement showing a rhombohedral cleavage, corroding detrital minerals (oligoclase, quartz), and filling available pore-space and fractures (Tables 1a, 1b) in Section L and Section LA. In some cases (L10), two generations of calcite cement have been detected.

Dolomite was detected in only one sample (sample LA1: 15%). As it has not been recognized in thin section, its textural relationships with other cements could not be determined.

Several samples of vitric tuff are reddened with hematite. In sample LA14B, hematite attains 47% (Table 1a). From optical microscopy, hematite cement fills all available pore-space and partially or totally occupies cracks and fractures. Hematite is also widespread throughout the altered vitric mass; its average grain-size (<5 μm) and euhedral shape are evident under the SEM (Fig. 7b). Iron became available owing to the hydrolysis of micas and glass during diagenesis.

The presence of sparitic calcite and ferric oxide impregnations along tubular pores (biological activity) and vertebrate remains (carbonate-rich fluorapatite) are all features found only in litharenites (sample LA14B) and correspond to an intereruptive facies (Manassero *et al*. 2000).

Halite has been detected by X-ray diffraction in some samples of both stratigraphic sections (Tables 1a, 1b) and by SEM in sample L12, where it shows dissolution features (Fig. 7c).

Trona [$Na_3H(CO_3)_2 \cdot 2H_2O$] has also been detected by X-ray diffraction in one sample (Table 1a), but its textural relationships with other minerals have not been observed.

Microcrystalline bipyramidal quartz cement (<5 μm) in the mesostasis of the tuffs is abundant in both sections and has been detected by SEM (Fig. 7d).

Minor proportions of chlorite (up to 5%, Table 1b) have been detected, as already reported by Cladera *et al*. (2004) in the sediments of the Cerro Castaño Member.

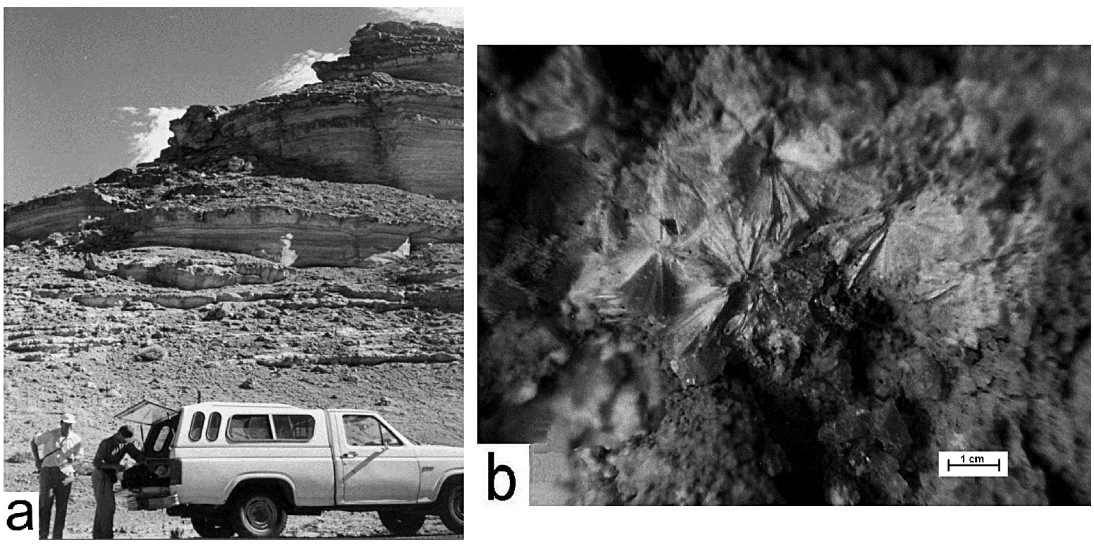

FIG. 3. a) Cerro Castaño Member outcropping in steep ridges. b) Dawsonite in rosette aggregates of whitish needles stained by ferric oxides.

Although anatase was detected in only one sample, it is interpreted here as the product of intense weathering.

The distribution of dawsonite

Although detailed studies on the tuffs of the Chubut Group have been carried out along the Middle Chubut River Valley (see Iñíguez Rodríguez *et al*. 1987, Iñíguez Rodríguez & Zalba 1992, Manassero *et al*. 1998, 2000, Cladera *et al*. 2004), no dawsonite had been found previously.

Restricted to two stratigraphic sections, near the Los Altares locality, in tuff and litharenite samples, dawsonite is present at the surface and in the interior of rocks. Its manifestation is limited to the middle and upper part of Section L, but it is spatially widespread and much more abundant in Section LA, averaging about 13% of the bulk rock.

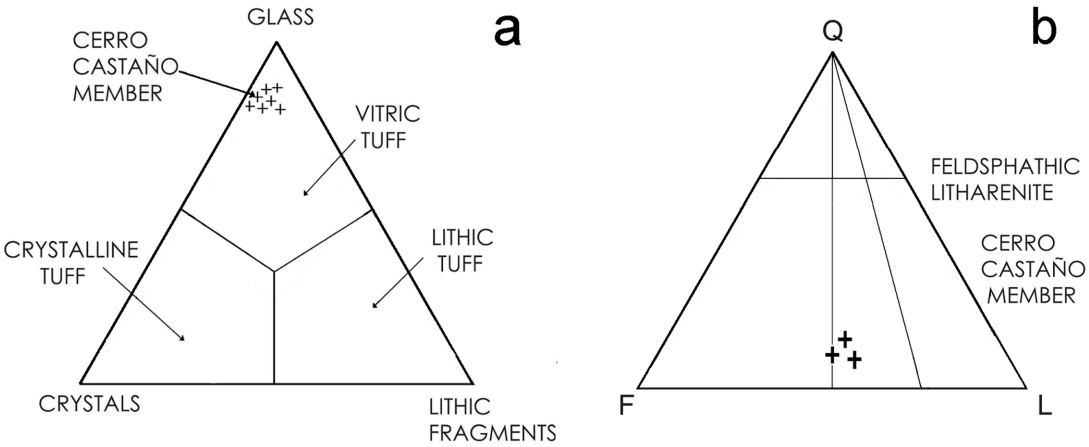

FIG. 4. a) Triangular diagram intended for the classification of tuffs of the Cerro Castaño Member (Pettijohn *et al*. 1987). b) Composition of fluvial interbedded sandstone plotted in the QFL diagram (Folk *et al*. 1970).

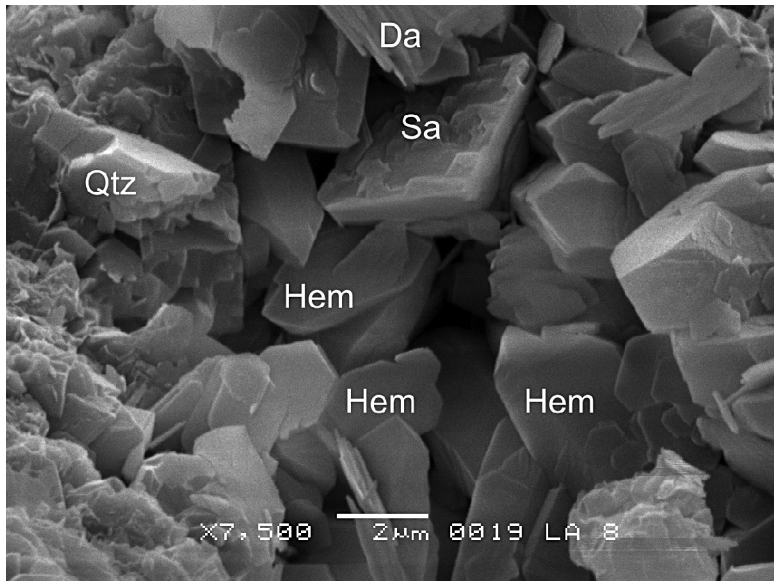

FIG. 5. SEM image of euhedral, prismatic crystals of high sanidine (Sa) associated with quartz (Qtz), dawsonite (Da) and hematite (Hem).

TABLE 1a. QUANTITATIVE PHASE-ANALYSIS OF SECTION LA (RIETVELD)

	LA1	LA2	LA3	LA4	LA5	LA6	LA7	LA8	LA9	LA10	LA11	LA12	LA13	LA14A	LA14B
Analcime				7.3				1.7		5.1		3.6			13.6
				0.3				0.2		0.2		0.2			0.2
Dawsonite	5.5	8.6		16.0	5.8	38.9	3.3	14.3	24.6	15.2	15.8	6.7	13.9	18.5	3.3
	0.4	0.4		0.10	0.4	0.19	0.5	0.7	0.12	0.8	0.7	0.4	0.6	0.9	0.5
Mica					4.2	3.7		1.8	n.c.	7.4		3.7		7.1	4.4
					0.2	0.4		0.2		0.2		0.2		0.3	0.3
Quartz	45.7	77.7	38.4	61.4	74.2	45.8	81.8	17.0	63.4	51.8	71.5	70.0	71.3	61.6	3.0
	0.5	0.7	0.3	0.9	0.6	0.10	0.7	0.3	0.11	0.7	0.7	0.5	0.6	0.8	0.2
Sanidine	20.4	9.6	60.5	10.4	6.5	1.0	11.3	4.8	5.2	11.8	6.4	13.7	9.5	7.4	2.6
	0.4	0.3	0.6	0.5	0.3	0.3	0.3	0.2	0.4	0.4	0.3	0.2	0.3	0.3	0.4
Oligoclase	8.5	1.3		4.8	6.3	10.4	3.6	1.0	6.6	5.3	4.5	2.4	1.7	5.4	5.0
	0.3	0.2		0.5	0.2	0.5	0.2	0.2	0.5	0.4	0.2	0.2	0.2	0.3	0.3
Calcite	4.6	2.8	1.1		3.0	<1		2.2	1.0				3.6		
	0.2	0.2	0.2		0.2			0.2	0.4				0.2		
Dolomite	15.2														
	0.2														
Halite								49.7		3.3	0.9				
								0.7		0.0.3	0.2				
Anatase											1.0				
											0.2				
Hematite															46.9
															0.8
C-Fap*															21.1
															0.2
Trona								7.5							
								0.2							

n.c.: not determined, * carbonate-rich fluorapatite. The modal proportions, with standard errors, are quoted in wt%.

TABLE 1b. QUANTITATIVE PHASE-ANALYSIS OF SECTION L (RIETVELD)

	L1	L2	L4	L5	L6	L7	L8	L10	L11	L12
Analcime	47.0	46.8	18.0	26.4	11.5	18.5	18.2	31.0	51.7	
	0.4	0.3	0.3	0.5	0.3	0.3	0.3	0.2	0.4	
Dawsonite						22.0				20.3
						0.5				0.5
Mica	3.9	4.5	4.5	32.8	30.2	5.2	5.1	4.1	3.9	
	0.2	0.3	0.2	0.13	0.12	0.3	0.3	0.2	0.2	
Quartz	23.7	40.8	60.0	15.6	40.8	42.6	50.3	48.7	32.3	70.5
	0.3	0.5	0.5	0.4	0.6	0.5	0.6	0.3	0.4	0.7
Sanidine	2.3	3.0	11.9	5.7	9.8	4.7	13.0	6.4	2.1	4.7
	0.3	0.3	0.3	0.4	0.3	0.3	0.3	0.2	0.2	0.3
Oligoclase	11.2	3.2	5.6	13.2	2.3	3.3	7.6	5.3	6.8	1.7
	0.2	0.2	0.2	0.3	0.2	0.2	0.2	0.2	0.2	0.3
Calcite	7.7	<1			2.6	3.7	3.0			
	0.3				0.3	0.3	0.3			
Chlorite	4.0	<1					2.8	4.5		2.7
	0.3						0.2	0.2		0.2
Halite				6.5	2.7				3.1	
				0.4	0.3				0.2	

The modal proportions, with standard errors, are quoted in wt%.

Description of the dawsonite

Macroscopically, dawsonite is easily distinguished by its white color, fine fibrous radial habit and silky luster (Fig. 3b). Outcrops of vitric tuffs of the Cerro Castaño Member show dawsonite in different modes of occurrence: a) on surface rocks, it appears as superficial whitish to pinkish aggregates of tiny needles (in some cases reddened with hematite) infilling cracks, oriented in several directions; b) radial aggregates of needles forming well-defined, coalescent rosettes up to 1 cm across preserved owing to the protection of overhanging strata.

Petrographic studies show a variety of textural relationships with coexisting authigenic phases in which dawsonite occurs: c) aggregates of radial needles replacing vitric masses (Fig. 8a); d) completely replacing pseudomorphically cuspate, planar, branching, Y-shaped or blebby glass shards (Fig. 8b); e) totally or partially replacing oligoclase (in some cases dawsonite replaces only one individual of a Carslbad-twinned crystal of oligoclase, Fig. 8c); f) partially replacing detrital quartz (see Fig. 6a); g) filling irregular cavities (Fig. 8d); and h) filling microcracks (Fig. 8d).

In our study of the paragenetic sequence through the SEM, striking mats of dawsonite fibers up to 1 mm long were found to grow over quartz cement (Fig. 8e).

The amounts of analcime and dawsonite display an inverse relationship (Tables 1a, 1b). Where analcime is abundant, dawsonite is absent (Section L), except for sample L7 where they coexist, almost equally represented. In Section LA, they may be present together, but with the increase in dawsonite, analcime decreases or disappears.

Although petrographic analyses show that oligoclase is commonly pseudomorphically replaced by dawsonite, in many cases (Fig. 8c) there is not a clear relationship between the amounts of the two minerals (Tables 1b, 1a).

Where calcite and dawsonite cements coexist, calcite is invariably subordinate to dawsonite. Textural relationships demonstrate that dawsonite fibers abut against calcite cement, and so, postdates it (Figs. 9a, b).

Hematite crystallized along both sides of microfractures, whereas dawsonite fills the center of them, which indicates that hematite predates the dawsonite (Fig. 9c).

The characterization of dawsonite

The unequivocal identification of hand-picked, almost pure, dawsonite was possible with X-ray diffraction (Fig. 10a). Almost all the reflections correspond to

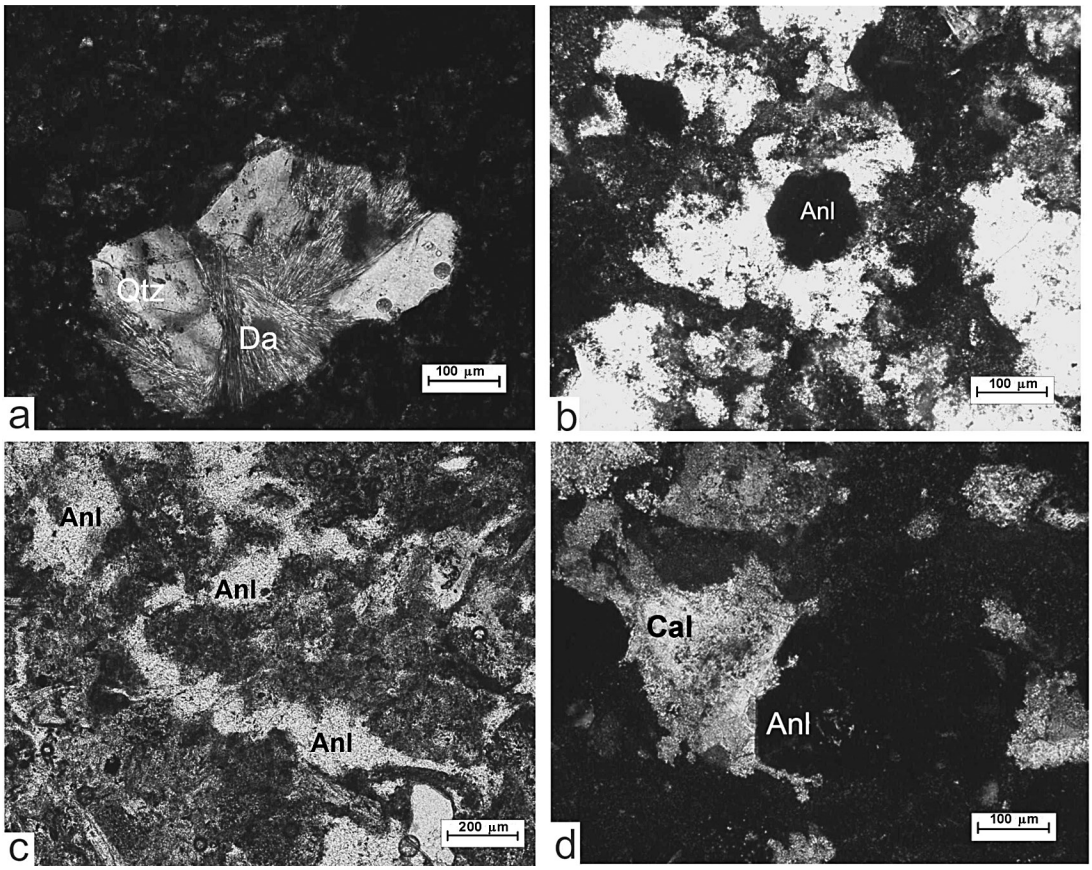

FIG. 6. Optical micrographs a) quartz (Qtz) grains partially corroded and replaced by dawsonite (Da). b) Euhedral crystals of analcime (Anl), c) Analcime (Anl) filling cavities and cracks. d) Textural relationship between analcime (Anl) and calcite (Cal) cement.

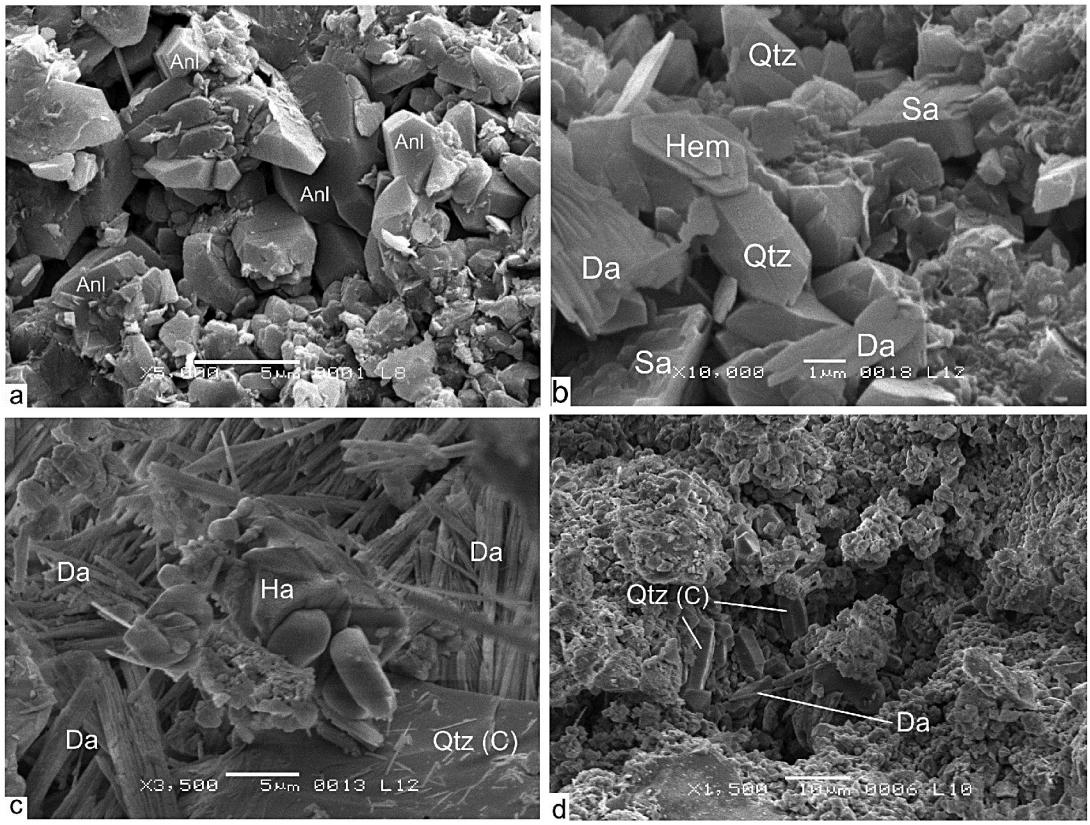

FIG. 7. SEM photos: a) Analcime (Anl) crystals with polyhedral forms (5 μm) and its distribution in the altered vitric mass. b) Hexagonal hematite (Hem) crystals associated with quartz (Qtz), dawsonite (Da) and high sanidine (Sa). c) Halite (Ha) with dissolution features, quartz (Qtz) and dawsonite (Da). d) Microcrystalline bipyramidal quartz (Qtz) cement (C) (<5 μm) and dawsonite (Da).

dawsonite; only traces of quartz are present as impurity. The cell parameters of dawsonite were calculated by the Rietveld refinement method, with initial data taken from Corazza *et al.* (1977). The unit-cell parameters are: *a* 6.759(3), *b* 5.587(4), *c* 10.423(4) Å. A quantitative estimation revealed up to 39% by weight (sample LA6, Table 1a). Dawsonite is by far more abundant in Section LA, being almost absent in Section L.

The thermal decomposition of dawsonite (Fig. 10b) can be represented by the following reaction:

$$NaAl(OH)_2CO_3 \rightarrow H_2O + CO_2 + NaAlO_2$$

The reaction corresponds to the description made by Huggins & Green (1973) as a two-step breakdown. An endothermic peak occurs between 287 and 525°C, and is related to a mass loss of 33.5%, indicating a loss of all the H_2O and part of the CO_2. The release of the remaining CO_2 and the recrystallization of the $NaAlO_2$ formed are represented by an exo–endo effect in the DTA curve and a mass loss of 8.2% between 525° and 700°C. The total mass-loss is 41.7%, resulting in a purity of 96.9%. The heated sampled was rapidly quenched in dry atmosphere and analyzed by X-ray diffraction. These analyses confirmed that all the residue is composed of $NaAlO_2$ and traces of quartz.

The results of a chemical analysis of the purified hand-picked sample are shown in Table 2, together with the theoretical values. The contents of Al_2O_3, Na_2O and the LOI indicate a very pure material.

Values of $\delta^{13}C$ and $\delta^{18}O$ for dawsonite of the Cerro Castaño Member tuffs and other isotopic data taken from the literature are plotted in Figure 11. Values of $\delta^{13}C$ are between –1.2 and –2.4‰. Values of $\delta^{18}O$ (SMOW) are from +13.9 to +15.2‰. A good concordance is found in the data from the two different laboratories where the analyses were performed (LABISE and INGEIS).

Discussion

Interpretation of mineral patterns

The analcime (average 5%) and quartz (between 15 and 20%) contents detected by petrographic analyses are coherent with results of other authors (Manassero *et al*. 2000, Cladera *et al*. 2004), but are significantly less than the amounts of these mineral phases detected by X-ray diffraction techniques (Tables 1a, 1b). This fact, as well as SEM observations, confirms the hypothesis that analcime (Fig. 7a) and most of the quartz (Fig.7d) are submicroscopic, mainly distributed in the sedimentary matrix and in secondary cavities, and of authigenic origin. Their formation within the matrix required

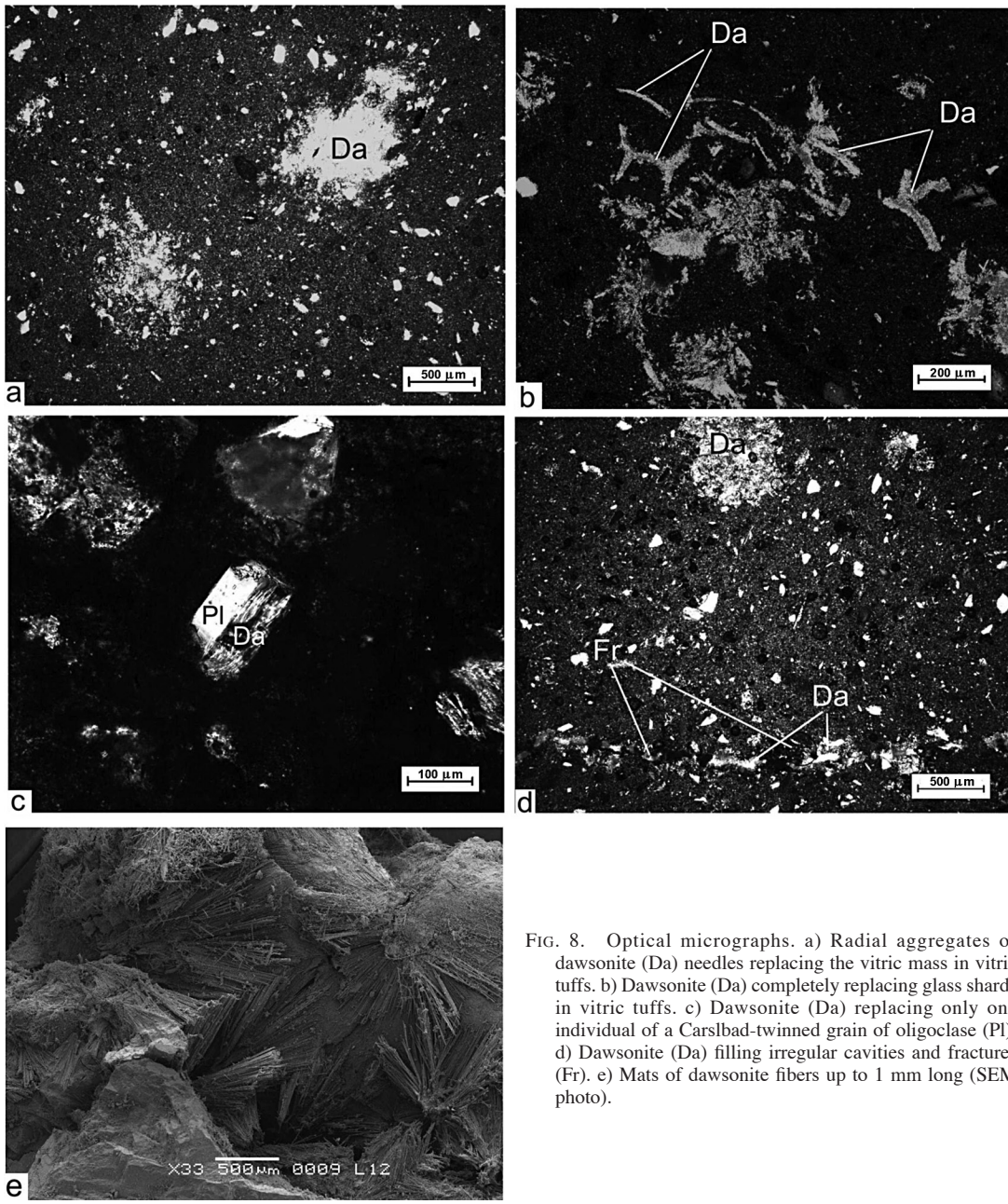

Fig. 8. Optical micrographs. a) Radial aggregates of dawsonite (Da) needles replacing the vitric mass in vitric tuffs. b) Dawsonite (Da) completely replacing glass shards in vitric tuffs. c) Dawsonite (Da) replacing only one individual of a Carslbad-twinned grain of oligoclase (Pl). d) Dawsonite (Da) filling irregular cavities and fractures (Fr). e) Mats of dawsonite fibers up to 1 mm long (SEM photo).

extended periods of impregnation of the deposits by saline alkaline solutions, as stated by Mees *et al*. (2005).

In the saline–alkaline lake environment, glass shards may transform by selective dissolution into smectite, and then, into clinoptilolite, phillipsite or erionite (Surdam 1977). As clinoptilolite was found in other stratigraphic sections of the Cerro Castaño Member (Iñíguez Rodríguez *et al*. 1987, Manassero *et al*. 2000, Cladera *et al*. 2004), it is reasonable to suppose that it acted as a silicic, alkaline precursor to analcime formed during burial diagenesis, as already proposed by Iñíguez Rodríguez *et al*. (1987).

From thin-section observations, the content of high sanidine rarely exceeds 5%, whereas a quantitative estimate through X-ray diffraction shows up to 60% of this mineral (Table 1a). The average size of the crystals (4–10 μm) explains the minor quantities obtained by Manassero *et al*. (2000) and Cladera *et al*. (2004) by optical microscopy, and also confirms that most of the high sanidine is distributed in the sedimentary matrix. The existence of high sanidine only, and no other K-feldspar in the tuffs, is interpreted in terms of a single origin for it. Euhedral, unaltered crystals of high sanidine coexisting with dawsonite cannot be attributed to a primary (igneous) origin owing to its instability when high alkaline, aggressive fluids interact with the host rocks, in this case to form dawsonite. Also, the unit-cell parameters are consistent with the group of anomalous alkali feldspar, of authigenic origin, in which *a* and *c* seem completely normal, but the *b* slightly departs from the series defined by homogeneous feldspars (Martin 1971). Accordingly, high sanidine is considered authigenic and postdating dawsonite and all other authigenic minerals.

Although calcite is not abundant, the presence of sparitic cement may account for breaks in (volcanic) sedimentation (Mees *et al*. 2005). Also, according to these authors, the presence of faunal activity, vertebrate remains and carbonate-rich fluorapatite found in litharenites may be related to subaerial exposures or soil formation during breaks in sedimentation (see also Cladera *et al*. 2004). In tuffs, calcite may have precipitated by evaporative concentration from groundwater in the capillarity zone where pH and the Mg:Ca ratio increase steadily as the groundwater moves toward the center of the basin (Surdam 1977).

A possible mechanism of dawsonite formation

The association analcime+dawsonite has only rarely been reported in the literature. Brobst & Tucker (1974) studied the composition and relationship of analcime with diagenetic dawsonite in tuffs of the Green River Formation. They concluded that analcime was converted to dawsonite under high partial pressures of CO_2 according to the reaction:

$$NaAlSi_2O_6 \cdot H_2O + CO_2 \leftrightarrow NaAlCO_3(OH)_2 + 2\,SiO_2$$
$$\text{Analcime} \leftrightarrow \text{Dawsonite} + \text{Quartz}$$

Loughnan & Goldbery (1972) stated that the occurrence of dawsonite in the Singleton Coal Measures of the Sydney Basin could be attributed to locally high partial pressures of CO_2. This statement is in agreement with Bader (1938), who proposed that considerable excess of CO_2 is necessary to precipitate dawsonite from solutions of sodium carbonate and sodium aluminate. Goldbery & Loughnan (1977) reported the occurrence of dawsonite in Permian marine strata of the Sydney Basin, Australia, which they interpreted to be of late syngenetic or epigenetic origin. Worden (2006) concluded that dawsonite in the Lam Formation, in Yemen, formed at expense of detrital plagioclase under conditions of elevated partial pressure of CO_2, with $\delta^{13}C$ about –4 to –2‰, and that it resulted from an influx of a magmatic CO_2 that pushed the Lam Formation into the stability field of dawsonite at the expense of albite in quartz-dominated sandstones.

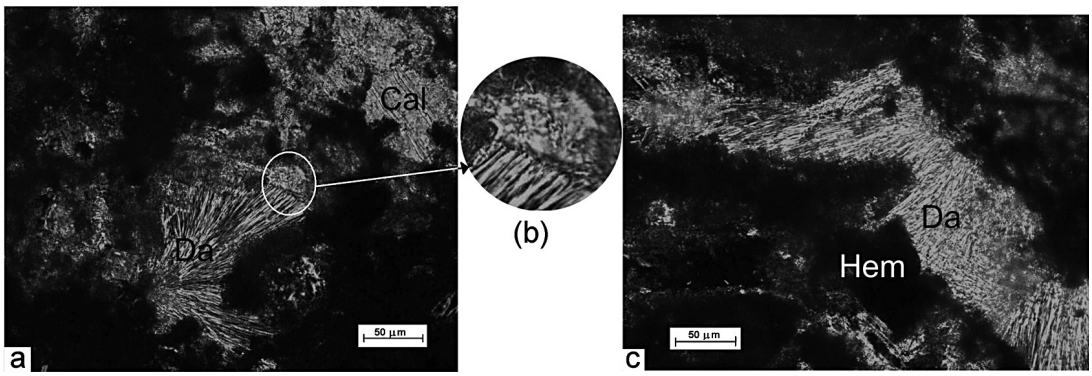

FIG. 9. Optical micrographs. a) Dawsonite (Da) fibers abutting against calcite (Cal) cement. b) Detail of photograph a. c) Hematite crystallized along both sides of microfractures.

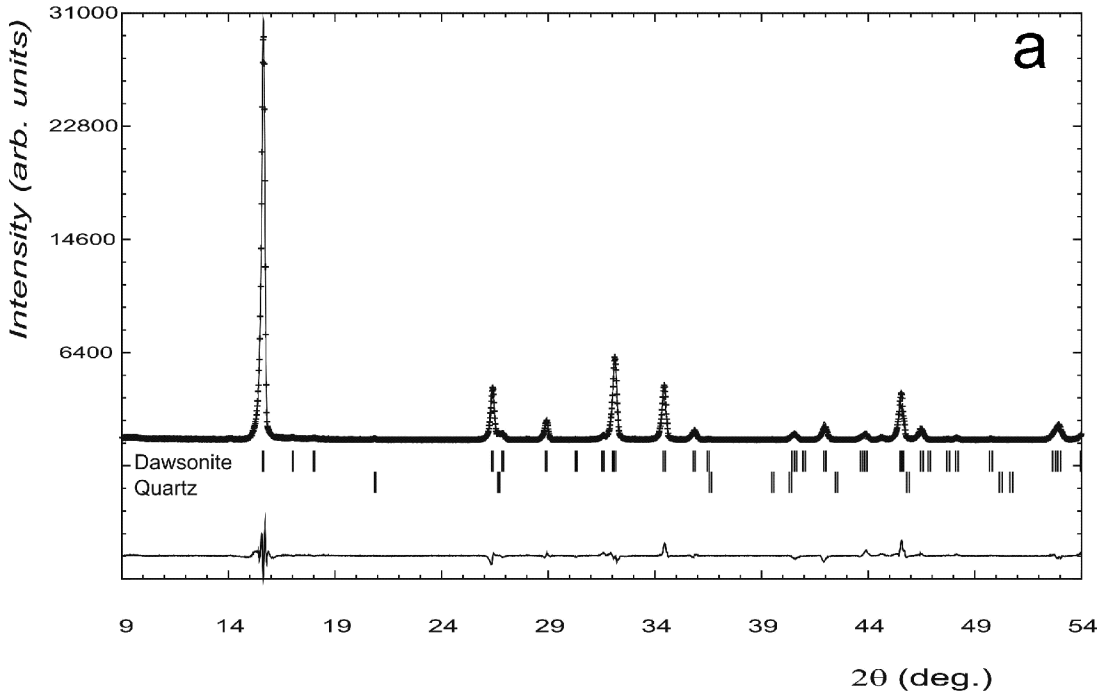

FIG. 10. a) X-ray diffractogram of hand-picked grains of dawsonite from vitric tuffs.

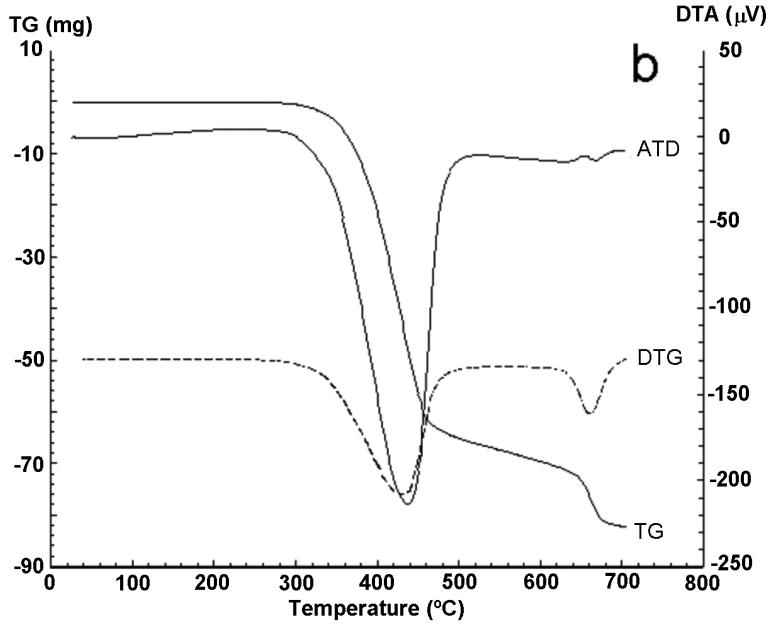

FIG. 10. b) Curves of the thermogravimetric and differential thermal analyses of dawsonite.

In the case of the deposits in the Cerro Castaño Member, an important factor to take into account concerning the mode and timing of formation of dawsonite is the inverse relationship between analcime and dawsonite, which points to a transformation of analcime into dawsonite as a reasonable hypothesis. Reference to this inverse relationship was made by Mason (1983). As the glass shards and vitric mass were previously replaced by analcime, as Iñíguez Rodríguez *et al*. (1987) demonstrated, it is realistic to suppose that analcime transformed into dawsonite, releasing silica to the system, according to the reaction proposed by Brobst & Tucker (1974) and mentioned above. The fact that dawsonite has replaced the vitric mass where analcime is concentrated is coherent with this assumption.

Dawsonite pseudomorphically replacing oligoclase and detrital quartz possibly implies that plagioclase and quartz dissolution occurred contemporaneously with dawsonite cementation.

The presence of dawsonite in fractures, its textural relationships with other diagenetic minerals, together with the fact that the fibers of dawsonite are not deformed or broken, imply not only the prior consolidation of the host sediments, but also the late appearance of dawsonite.

The paleoenvironment of deposition

The Chubut Group was deposited in semigrabens with a thickness of more than 1000 m of sediments (ash fall tuffs) in alluvial plains associated with saline–alkaline lakes (Iñíguez Rodríguez *et al*. 1987, Manassero *et al*. 2000). Diverse geological features described for these lacustrine deposits (Sheppard & Gude 1968, Hay

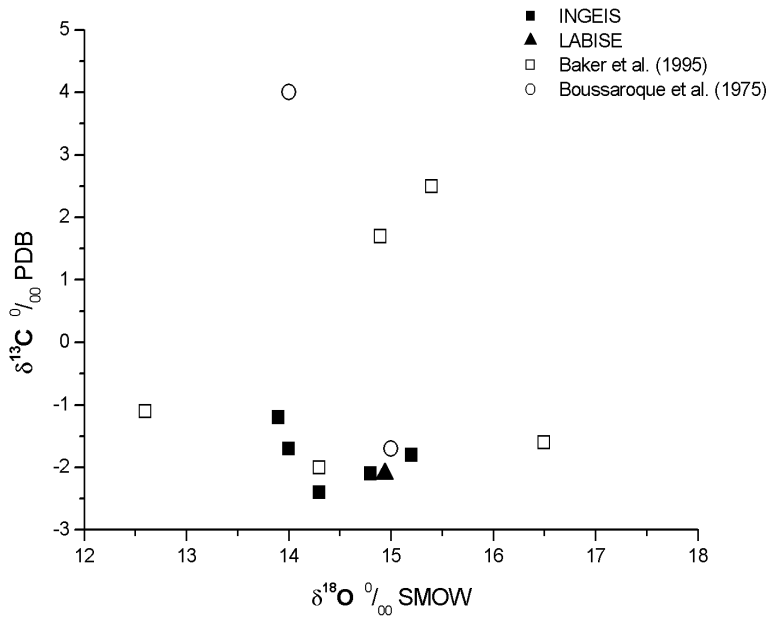

FIG. 11. Stable isotope data, $\delta^{13}C$ and $\delta^{18}O$, for dawsonite of the Cerro Castaño Member tuffs. Values are also plotted for other examples of magmatic dawsonite taken from Boussaroque *et al*. (1975) and from Baker *et al*. (1995).

TABLE 2. CHEMICAL COMPOSITION OF HAND-PICKED DAWSONITE (1) COMPARED WITH THE THEORETICAL COMPOSITION (2)

	SiO_2	Al_2O_3	Fe_2O_3	MnO	MgO	CaO	Na_2O	K_2O	TiO_2	P_2O_5	LOI
(1)	0.79	35.08	0.08	0	0.02	0.10	20.80	0.02	0	0.02	42.66
(2)	-	35.4	-	-	-	-	21.5	-	-	-	42.9*

LOI: Loss on ignition, * $H_2O + CO_2$. Concentrations are reported in wt%.

1977, Surdam 1977) have also been found among the different members of the Cerro Barcino Formation (Musachio & Chebli 1975, Iñíguez Rodríguez *et al*. 1987, Manassero *et al*. 2000, Cladera *et al*. 2004). The hypothesis that the deposits studied here correspond to the central part of saline–alkaline lakes, where salinity and alkalinity of the connate waters are higher than in the outer zones, is reasonable on the basis of the presence of diagenetic halite and trona.

According to the interpretation of mineral patterns and textural relationships, we document a late diagenetic stage of formation of dawsonite (Fig. 12). We contend that several generations of silica cement were released to the system, and that compaction may have occurred after the formation of zeolite and some generations of silica, because they crystallized filling available pore-space and cavities and are not deformed, but probably before hematite, halite and trona cementation. The presence of two generations of calcite cement may correspond to two different geological environments, with the second one, affecting etched quartz, occurring after dissolution of quartz and oligoclase.

The origin of CO_2, Na and Al

We agree with Loughnan & Goldbery (1972) that fluids with high partial pressures of CO_2 (and not pH) must have promoted the formation of dawsonite, because of the minor occurrence of associated analcime. The CO_2-rich fluids must have migrated through fractures and faults related to the semigrabens. This assumption is explained by the accompanying zeolitization and partial silicification, which occurred prior to the formation of dawsonite during burial diagenesis of the sediments, reducing their permeability and porosity, and turning these deposits into a confining unit capable of retaining CO_2-rich fluids.

Fluids rich in CO_2 are likely to derive from magmatic sources, *i.e.,* hypabyssal alkaline intrusive bodies (Los Buitres – El Canquel Formation) emplaced along NW- and NE-trending lineaments and fractures reactivated during Eocene–Miocene time (Anselmi *et al*. 2004). These bodies are found less than 10 km away in the area and cross-cut the Cerro Barcino Formation. This argument is consistent with the values of $\delta^{13}C$ (–1.7 to –2.4‰) obtained here from almost pure dawsonite samples, which are in accordance with a magmatic origin, being found in other parts of the world (Boussaroque *et al*. 1975, Baker *et al*. 1995, see Fig. 11). Also, isotopic data presented by Golab *et al*. (2006) and Worden (2006) for the source of magmatic carbon for dawsonite from the Sydney and Shabwa basins, respectively, are comparable to those from the Cerro Castaño dawsonite. Moreover, deep sources of CO_2, common in tectonically active areas of the world, have $\delta^{13}C$ values of about –6 ± 2‰ PDB, and are related with igneous activity or deep-seated faults, according to Ohmoto & Rye (1979). In accordance with the arguments presented above, our isotopic data are inconsistent with a marine origin or one involving organic matter for the source of the CO_2.

Values of $\delta^{18}O$ are coherent with the data presented by Baker *et al*. (1995). We can thus assume that the oxygen is not of meteoric origin. In light of this evidence, dawsonite could not be older than Eocene.

The formation of dawsonite from analcime implies the release of SiO_2 during the reaction. Manassero *et al*. (2000) proposed that the chemical composition of the tuffs reflects the composition of the parental rhyolitic magma, although the intense diagenetic silicification makes it difficult to identify its precise source. Probably there have been several episodes of silicification, at different stages of diagenesis, in view of the chemical reactions involved during the transformation of glass shards to smectite, clinoptilolite, analcime and, finally, dawsonite, all of which release SiO_2 to the environment as a byproduct.

As oligoclase has been totally or partly replaced by dawsonite in the Cerro Castaño Member, the released Al and Na must have, to some extent, contributed to its formation which then, must have been contemporaneous. Coveney & Kelly (1971) have proposed two chemical reactions of plagioclase to give dawsonite in the presence of high partial pressure of CO_2 and H_2O.

$$\underset{\text{Albite}}{NaAlSi_3O_8} + H_2O + CO_2 \leftrightarrow 3\,\underset{\text{Quartz}}{SiO_2} + \underset{\text{Dawsonite}}{NaAlCO_3(OH)_2}$$

$$\underset{\text{Oligoclase}}{Na_9CaAlSi_{29}O_{80}} + 11\,H_2O + 11\,CO_2 + 2\,Na^+ \leftrightarrow 29\,\underset{\text{Quartz}}{SiO_2} + 11\,\underset{\text{Dawsonite}}{NaAlCO_3(OH)_2} + Ca^{2+}$$

Pyroclastic material (shards) did not contribute Na and Al to the formation of dawsonite, because shards had already been transformed to analcime by the time the dawsonite formed. Apart from considering oligoclase and analcime as internal sources of Na for dawsonite development, the principal external source for Na and Al probably derived from hydrothermal fluids provided by alkaline hypabyssal bodies during Eocene time. This is coherent with textural descriptions showing that dawsonite is independent of sedimentary facies (it appears in tuffs and litharenites as well). As was previously stated, analcime in Section L is found mostly replacing vitric masses; consequently, the hypothesis that also vitric masses were already transformed to analcime, previous to the formation of dawsonite in Section LA, is a realistic one. This supposition would clarify the observation that "minor occurrence of analcime associated with dawsonite is found in the Singleton Coal Measures of the Sydney Basin" (Loughnan & Goldbery 1972), because dawsonite was formed at the expense of analcime. The virtual absence of analcime in Section LA with respect to Section L would also be consistent with this inference.

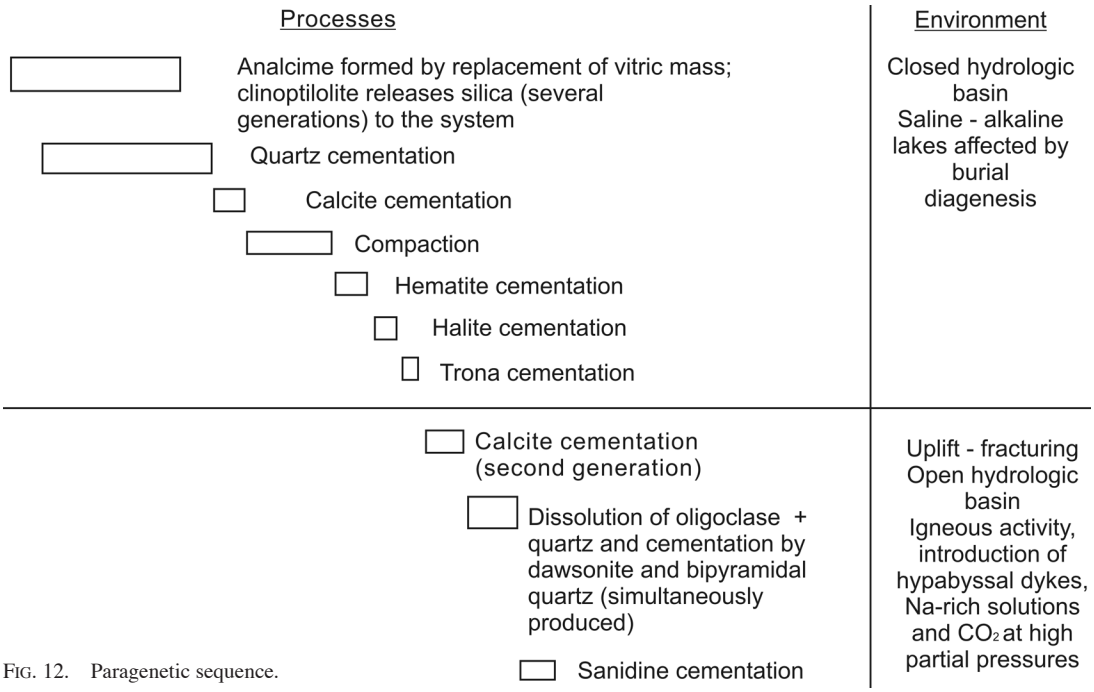

FIG. 12. Paragenetic sequence.

CONCLUSIONS

1. Dawsonite has been identified in vitric tuffs and litharenites of the Cerro Castaño Member, Chubut Group, in the Middle Valley of the Chubut River.

2. These rocks, deposited in saline–alkaline lake paleoenvironments (closed hydrologic basin), experienced burial diagenesis. By hydrolysis, the vitric glass was transformed into clay minerals, then to analcime *via* a more silicic zeolite (clinoptilolite), released silica to the environment as a by-product in different episodes of chemical reactions, followed by the precipitation of calcite, hematite, halite and trona. Silicification decreased the porosity and permeability of the unit.

3. Uplift and fracturing during Eocene time led to the intrusion of basic alkaline hypabyssal dykes (El Buitre – El Canquel Formation), which provided external high partial pressures of CO_2 and Na-rich fluids (attack on hydroaluminosilicates) for dawsonite formation. An internal source of Na and Al for dawsonite formation was provided by the transformation of analcime and oligoclase, which occurred contemporaneously with the generation of dawsonite.

4. The $\delta^{13}C$ PDB values (–1.7 to – 2.4‰) of dawsonite are interpreted as being derived from a magmatic source, whereas from the $\delta^{18}O$ SMOW values (+13.9 to +15.2‰), it can be assumed that the oxygen is not of meteoric but rather of diagenetic origin.

5. Dawsonite postdated all other cements generated except the unaltered crystals of high sanidine.

ACKNOWLEDGEMENTS

This study was supported by the Comisión de Investigaciones Científicas de la provincia de Buenos Aires and by the Centro de Tecnología de Recursos Minerales y Cerámica (CETMIC), Argentina. We are grateful to Dr. A.N. Sial from the Laboratorio de Isotopos Estáveis (LABISE), Universidade Federal de Pernambuco, Recife, Brazil, for isotopic analyses. The authors thank referee M.F. Marquez-Zavalía and Associate Editor Dr. D. Mossman for their critical review and comments, which allowed us to improve the paper. We are grateful for the review and valuable suggestions of the editor, Dr. Robert F. Martin.

REFERENCES

ANSELMI, G., GAMBA, M.T. & PANZA, J.L. (2004): Hoja Geológica 4369–IV, Los Altares. Provincia del Chubut. *Servicio Geológico Minero Argentino* **313**, 1-98.

ANSELMI, G., PANZA, J.L., CORTÉS, J.M. & RAGONA, D. (2000): Hoja Geológica N° 4569–II, El Sombrero, Provincia del Chubut. *Servicio Geológico Minero Argentino* **271**, 1-87.

ARDOLINO, A.A., BUSTEROS, A., CUCCHI, R., FRANCHI, M., LEMA, H. & REMESAL, M. (1995): Cuerpos alcalinos

básicos paleógenos del sur de Somún Curá (Argentina) y su marco estratigráfico. *Ameghiniana, Asociatión Paleontológica Argentina, Publicación Especial* **3**, 7-22.

BADER, E. (1938): Über die Bildung und Konstitution des Dawsonit und seine synthetische Darstellung. *Neues Jahrb. Mineral. Geol. Paläont.* **74**, 449-465.

BAKER, J.C. (1991): Diagenesis and reservoir quality of the Aldebaran Sandstone, Denison Trough, east-central Queensland. Australia. *Sedimentology* **38**, 819-838.

BAKER, J.C., BAI, G.P., HAMILTON, P.J., GOLDING, S.D. & KEENE, J.B. (1995): Continental-scale magmatic carbon dioxide seepage recorded by dawsonite in the Bowen–Gunnedah–Sydney Basin system, eastern Australia, *J. Sedim. Res.* **A65**, 522-530.

BARCAT, C., CORTIÑAS, S., NEVISTIC, V.A. & ZUCHI, H.E. (1989): Cuenca Golfo San Jorge. *In* Cuencas Sedimentarias Argentinas (G.A. Chebli, & L.A. Spalletti, eds.). *Instituto Superior de Correlación Geológica, Universidad Nacional de Tucumán*, *Serie de Correlación Geológica* **6**, 319-345.

BISH, D.L. & POST, J.E. (1993): Quantitative mineralogical analysis using the Rietveld full-pattern fitting method. *Am. Mineral.* **78**, 932-940.

BOUSSAROQUE, J., LÉTOLLE, R. & MAURY, R. (1975): Formation de la dawsonite des Richât (Adrar de Mauritanie): analyse isotopique ^{13}C et ^{18}O. *C.R. Acad. Sci. Paris* **281**, *sér.* **D**, 1075-1078.

BROBST, D.A. & TUCKER, J.D. (1974): Composition and relation of analcime to diagenetic dawsonite in oil shale and tuff in the Green River Formation, Piceance Creek basin, northwestern Colorado. *J. Res. U.S. Geol. Surv.* **2**, 35-39.

CHEBLI, G.A., NAKAYAMA, C., SCIUTTO J.C. & SERRAIOTTO, A.A. (1976): Estratigrafía del Grupo Chubut en la región central de la provincia homónima. *Actas VI Congreso Geológico Argentino* **1**, 375-392.

CLADERA, G., LIMARINO, C.O., ALONSO, M.S. & RAUHUT, O.W.M. (2004): Controles estratigráficos en la preservación de restos de vertebrados en la Formación Cerro Barcino (Cenomaniano), Provincia del Chubut. *Revista de la Asociación Argentina de Sedimentología* **11**(2), 39-56.

CODIGNOTTO, J., NULLO, F., PANZA, J. & PROSERPIO, C. (1978): Estratigrafía del Grupo Chubut, entre Paso de Indios y Las Plumas, Provincia del Chubut. *Actas VII Congreso Geológico Argentino* (*Neuquén*), **1**, 471-480.

COPLEN, T.B. (1994): Reporting of stable hydrogen, carbon, and oxygen isotopic abundances. *Pure Appl. Chem.* **66**, 273-276.

CORAZZA, E., SABELLI, C. & VANNUCCI, S. (1977): Dawsonite: new mineral data and structure refinement. *Neues Jahrb. Mineral., Monatsh.,* 381-397.

COVENEY, R.M. & KELLY, W.C. (1971): Dawsonite as a daughter mineral in hydrothermal fluid inclusions. *Contrib. Mineral. Petrol.* **32**, 334-342.

DOMÍNGUEZ, E. & GÓMEZ, C. (1988): El régimen hidrotermal de la mina Erika, Andacollo, Provincia de Neuquén. *Revista de la Asociación Geológica Argentina* **43**(1), 24-42.

FERNÁNDEZ, M. (2000): Descripción petrográfica de muestras correspondientes a la Hoja Geológica 4369 IV Los Altares, Provincia del Chubut. *Servicio Geológico Minero Argentino*, *Unpubl. Rep.* **3372**, 1-20.

FISHER, R.V. & SCHMINCKE, H.U. (1984): *Pyroclastic Rocks*. Springer-Verlag, Berlin, Germany.

FITZGERALD, M.G., MITCHUM, R.M., ULIANA, M.A. & BIDDLE, K.T. (1990): Evolution of the San Jorge Basin, Argentina. *Am. Assoc. Petrol. Geol. Bull.* **74**, 879-920.

FOLK, R.L., ANDREWS, P.B. & LEWIS, D.W. (1970): Detrital sedimentary rock classification and nomenclature for use in New Zealand. *N.Z. J. Geol. Geophys.* **13**, 937-968.

GOLAB, A.N., CARR, P.F. & PALAMARA, D.R. (2006): Influence of localised igneous activity on cleat dawsonite formation in Late Permian coal measures, Upper Hunter Valley, Australia. *Int. J. Coal Geol.* **66**, 296-304.

GOLDBERY, R. & LOUGHNAN, F.C. (1970): Dawsonite and nordstrandite in the Permian Berry Formation of the Sydney Basin, New South Wales. *Am. Mineral.* **55**, 477-490.

GOLDBERY, R. & LOUGHNAN, F.C. (1977): Dawsonite, alumohydrocalcite, nordstrandite and gorceixite in Permian marine strata of the Sydney Basin, Australia. *Sedimentology* **24**, 565-579.

HAY, R.L. (1963): Zeolitic weathering in Olduvai Gorge, Tanganyika. *Geol. Soc. Am., Bull.,* **74**, 1281-1286.

HAY, R.L. (1964): Phillipsite of saline lakes and soils. *Am. Mineral.* **49**, 1366-1387.

HAY, R.L. (1977): Geology of zeolites in sedimentary rocks. *In* Mineralogy and Geology of Natural Zeolites (F.A. Mumpton, ed.). *Rev. Mineral.* **4**, 53-64.

HUGGINS, C.W. & GREEN, T.E. (1973): Thermal decomposition of dawsonite. *Am. Mineral.* **58**, 548-550.

IÑÍGUEZ RODRÍGUEZ, A.M. & ZALBA, P.E. (1992): Zeolitas del Grupo Chubut (Cretácico), Provincia de Chubut, Argentina. *In* Zeolitas '91. Memorias de la III Conferencia Internacional sobre Ocurrencia, Propriedades y Usos de las Zeolitas Naturales. Edición de la Academia de Ciencias de Cuba **1**, 43-48.

IÑÍGUEZ RODRÍGUEZ, A.M., ZALBA, P.E. & MAGGI, J.H. (1987): Clinoptilolita y analcima en miembros del Grupo Chubut, entre Paso de Indios y Las Plumas, Provincia de Chubut, Argentina. *Actas X Congreso Geológico Argentino* (*Tucumán*) **1**, 75-78.

KASTNER, M. (1971): Authigenic feldspars in carbonate rocks. *Am. Mineral.* **56**, 1403-1442.

KAY, S.M., ARDOLINO, A.A., FRANCHI, M. & RAMOS, V.A. (1993): El origen de la meseta de Somún Curá: distribución y geoquímica de sus rocas volcánicas máficas. *Actas XII Congreso Geológico Argentino* (*Mendoza*) **4**, 236-248.

LEMA, H.A. & CORTÉS, J.M. (1987): El vulcanismo eoceno del flanco oriental de la Meseta del Canquel, Chubut, Argentina. *Actas X Congreso Geológico Argentino* (*Tucumán*) **4**, 188-191.

LESTA, P.J. & FERELLO, R. (1972): Región extraandina de Chubut y norte de Santa Cruz. *In* Geología Regional Argentina (A.F. Leanza, ed.). Academia Nacional de Ciencias de Córdoba, 601-653.

LOUGHNAN, F.C. & GOLDBERY, R. (1972): Dawsonite and analcite in the Singleton Coal Measures of the Sydney Basin. *Am. Mineral.* **57**, 1437-1447.

LOUGHNAN, F.C. & SEE, G.T. (1967): Dawsonite in the Greta Coal Measures at Muswellbrook, New South Wales. *Am. Mineral.* **52**, 12l6-1219.

MANASSERO, M.L. (1997): Sedimentology of the Upper Cretaceous Red Beds of Angostura Colorada Formation in the western sector of the Northpatagonian Massif, Argentina. *J. S. Am. Earth Sci.* **10**, 81-90.

MANASSERO, M., ZALBA, P.E., ANDREIS, R.R & MOROSI, M. (1998): Ambientes volcaniclásticos de la Formación Cerro Barcino (Grupo Chubut, Cretácico Superior) entre la localidad de Los Altares y Las Plumas, Chubut, Argentina. *Actas VII Reunión Argentina de Sedimentología* (*Salta*), 268-279.

MANASSERO, M., ZALBA, P.E., ANDREIS, R.R. & MOROSI, M. (2000): Petrology of continental pyroclastic and epiclastic sequences in the Chubut Group (Cretaceous): Los Altares – Las Plumas area, Chubut, Patagonia, Argentina. *Revista Geológica de Chile* **27**, 13-26.

MARTIN, R.F. (1971): Disordered authigenic feldspars of the series $KAlSi_3O_8$–$KBSi_3O_8$ from southern California. *Am. Mineral.* **56**, 281-291.

MASON, G.M. (1983): Mineralogy of the Mahogany Marker Tuff of the Green River Formation, Piceance Creek Basin, Colorado. *In* Proceedings of the Sixteenth Oil Shale Symposium (J.H. Gary, ed.). Colorado School of Mines, Golden, Colorado (124-131).

MCCREA, J.M. (1950): On the isotopic chemistry of carbonates and a paleotemperature scale. *J. Chem. Phys.* **18**, 849-857.

MEES, F., STOOPS, G., VAN RANST, E., PAEPE, R. & VAN OVERLOOP, E. (2005): The nature of zeolite occurrences in deposits of the Olduvai Basin, northern Tanzania. *Clays Clay Minerals* **53**, 659-673.

MUSACCHIO, E.A. (1972): Carófitas del Cretácico inferior en sedimentitas chubutenses al Este de la Herrería, Chubut. *Ameghiniana* **9**(4), 354-356.

MUSACCHIO, E.A. & CHEBLI, G. (1975): Ostrácodos no marinos y carófitos del Cretácico Inferior en las Provincias del Chubut y Neuquén, Argentina. *Ameghiniana* **12**(1), 70-96.

OHMOTO, H. & RYE, R.O. (1979): Isotopes of sulphur and carbon. *In* Geochemistry of Hydrothermal Ore Deposits (second edition; H.L. Barnes, ed.). John Wiley & Sons, New York, N.Y. (509-567).

PETTIJOHN, F.J., POTTER, P.E. & SIEVER, R. (1987): *Sand and Sandstone*. Springer Verlag, New York, N.Y.

RIETVELD, H.M. (1969): A profile refinement method for nuclear and magnetic structures. *J. Appl. Crystallogr.* **2**, 65-71.

ROBBIANO, J. (1971): Contribución al conocimiento estratigráfico de la Sierra del Cerro Negro, Pampa de Agnia, Provincia de Chubut, República Argentina. *Revista de la Asociación Geológica Argentina* **26**(1), 41-56.

RODRÍGUEZ CARVAJAL, J. (2001): Recent Developments of the Program FULLPROF. *Commission on Powder Diffraction* (IUCr), *Newsletter* **26**, 12-19.

SHEPPARD, R.A. & GUDE, A.J., II (1968): Distribution and genesis of authigenic silicate minerals in tuffs of the Pleistocene Lake Tecopa, Inyo County, California. *U.S. Geol. Surv., Prof. Pap.* **597**.

SMITH, J.W. & MILTON, C. (1966): Dawsonite in the Green River Formation of Colorado. *Econ. Geol.* **61**, 1029-1042.

STEVENSON, J.S. & STEVENSON, L.S. (1977): Dawsonite–fluorite relationships at Montreal-area localities. *Can. Mineral.* **15**, 117-120.

STEVENSON, J.S. & STEVENSON, L.S. (1978): Contrasting dawsonite occurrences from Mont St-Bruno, Quebec. *Can. Mineral.* **16**, 471-474.

SURDAM, R.C. (1977): Zeolites in closed hydrologic systems. *In* Mineralogy and Geology of Natural Zeolites (F.A. Mumpton, ed.). *Rev. Mineral.* **4**, 65-91.

VOLKHEIMER, W. (1969): Problemas del Grupo Chubut. *Ameghiniana* **6**(2), 173-180.

WORDEN, R.H. (2006): Dawsonite cement in the Triassic Lam Formation, Shabwa Basin, Yemen: a natural analogue for a potential mineral product of subsurface CO_2 storage for greenhouse gas reduction. *Mar. Petrol. Geol.* **23**, 61-77.

WRIGHT, T.L. & STEWART, D.B. (1968): X-ray and optical study of alkali feldspar. I. Determination of composition and structural state from refined unit-cell parameters and 2V. *Am. Mineral.* **53**, 38-87.

Received April 27, 2010, revised manuscript accepted April 22, 2011.